

Assembly of Three Cadmium(II) Complexes Based on Flexible α,ω -Bis(benzimidazolyl)alkane Ligands

Jian-Chen Geng, Cui-Huan Jiao, Jin-Ming Hao, and Guang-Hua Cui

College of Chemical Engineering, Hebei United University, 46 West Xinhua Road, Tangshan 063009, Hebei, P. R. China

Reprint requests to Prof. G.-H. Cui. E-mail: tscghua@126.com

Z. Naturforsch. **2012**, 67b, 791–798 / DOI: 10.5560/ZNB.2012-0158

Received June 10, 2012

Three flexible α,ω -bis(5,6-dimethylbenzimidazolyl)alkane ligands with different spacers were reacted with CdX_2 ($X = \text{Cl}, \text{Br}, \text{I}$) hydrothermally, resulting in three coordination architectures, namely $[\text{CdI}_2(\text{L}^1)]_n$ (**1**), $[\text{CdBr}_2(\text{L}^2)]_n$ (**2**), and $\text{Cd}_2\text{Cl}_4(\text{L}^3)_2$ (**3**) [$\text{L}^1 = 1,3$ -bis(5,6-dimethylbenzimidazole)propane, $\text{L}^2 = 1,5$ -bis(5,6-dimethylbenzimidazole)pentane, $\text{L}^3 = 1,6$ -bis(5,6-dimethylbenzimidazole)hexane]. They have been characterized by elemental analyses, IR spectra, thermogravimetric (TG) analysis, and single-crystal X-ray diffraction. Complex **1** displays a helical chain linked by the ligands L^1 , and a 2D supramolecular network is constructed through $\pi-\pi$ stacking interactions; complex **2** shows a helical chain structure with connections through two kinds of strong $\pi-\pi$ stacking interactions into an intricate 3D supramolecular network; complex **3** contains dinuclear metallomacrocycles. The fluorescence properties of **1–3** have been investigated in the solid state.

Key words: α,ω -Bis(5,6-dimethylbenzimidazolyl)alkanes, Cadmium(II), Different Spacers, Fluorescence Properties

Introduction

The construction of coordination polymers and networks by self-assembly of organic ligands and appropriate metal ions is a rapidly growing area of research, not only for their remarkable potential applications in luminescence, redox activity and magnetism, but also for their intriguing variety of molecular architectures and topologies [1–7]. As for organic ligands, variable molecular backbones and functional groups promote the adjustable assembly of coordination polymer networks. Among the N -donor ligands with multidentate systems, flexible α,ω -bis(benzimidazolyl)alkane ligands have proved to be useful ligands for metal ions, due to their reactivity and adaptability in the stabilization of diverse structures and with versatile biological activity [8–17]. The organic spacers play a role in the structural tuning of the resulting polymers. The spatially extended directionality and the conformational preference provided by the ligands containing alkyl spacers can result in a remarkable class of polymers with diverse architectures and functions [18, 19].

Among the series of benzimidazole derivatives, the most prominent compound is 5,6-dimethylbenzimidazole, which serves as an axial ligand for cobalt in vitamin B_{12} [20]. Herein, we use a series of α,ω -bis(5,6-dimethylbenzimidazolyl)alkanes as flexible bridging ligands which can provide more information on the influence of methyl substituents on the structures and properties of the resulting complexes. This type of coordination polymers have only been scarcely studied [21–25].

Results and Discussion

The crystal and molecular structures of complexes **1–3** were determined. Table 1 summarizes the crystallographic data and experimental details of data collection and structure refinement. Selected bond lengths and angles for **1–3** are listed in Table 2.

Crystal structure of $[\text{CdI}_2(\text{L}^1)]_n$ (**1**)

Single-crystal structure analysis shows that **1** crystallizes in the monoclinic space group $P2_1/c$ with

Complex	1	2	3
Empirical formula	C ₂₁ H ₂₄ CdI ₂ N ₄	C ₂₃ H ₂₈ Br ₂ CdN ₄	C ₄₈ H ₆₀ Cd ₂ Cl ₄ N ₈
Formula weight	698.64	632.71	1115.66
Crystal size, mm ³	0.11 × 0.12 × 0.08	0.20 × 0.19 × 0.19	0.15 × 0.14 × 0.14
Crystal system	monoclinic	monoclinic	monoclinic
Space group	<i>P</i> 2 ₁ / <i>c</i>	<i>P</i> 2 ₁ / <i>c</i>	<i>P</i> 2 ₁ / <i>n</i>
<i>a</i> , Å	10.9057(5)	10.2302(7)	10.9503(7)
<i>b</i> , Å	14.5648(7)	17.1414(12)	14.3080(9)
<i>c</i> , Å	15.9285(7)	14.7536(10)	16.1625(11)
β , deg	113.526(3)	100.1870(10)	98.2250(10)
<i>V</i> , Å ³	2319.77(18)	2546.4(3)	2506.2(3)
<i>Z</i>	4	4	2
<i>D</i> _{calcd} , g cm ⁻³	2.00	1.65	1.48
<i>F</i> (000), e	1328	1248	1136
<i>T</i> , K	298(2)	298(2)	298(2)
<i>hkl</i> range	±12, ±17, ±18	±12, ±20, ±17	−12 → 13, −16 → 17, ±19
Refl. measd./unique	17 382/4082	19 201/4489	18 866/4424
<i>R</i> _{int}	0.0234	0.0380	0.0476
μ (Mo <i>K</i> α), mm ⁻¹	3.6	4.0	1.1
<i>R</i> ₁ / <i>wR</i> ₂ [<i>I</i> > 2 σ (<i>I</i>)] ^{a,b}	0.0691/0.2199	0.0448/0.1121	0.0358/0.0841
<i>R</i> ₁ / <i>wR</i> ₂ (all data) ^{a,b}	0.0754/0.2264	0.0747/0.1274	0.0565/0.0948
GoF (<i>F</i> ²) ^c	1.060	1.048	1.029
$\Delta\rho_{\text{fin}}$ (max/min), e Å ⁻³	2.89/−2.51	0.82/−0.79	0.68/−0.32

^a $R_1 = \Sigma ||F_o| - |F_c|| / \Sigma |F_o|$; ^b $wR_2 = [\Sigma w(F_o^2 - F_c^2)^2 / \Sigma w(F_o^2)^2]^{1/2}$, $w = [\sigma^2(F_o^2) + (AP)^2 + BP]^{-1}$, where $P = (\text{Max}(F_o^2, 0) + 2F_c^2)/3$; ^c GoF = $[\Sigma w(F_o^2 - F_c^2)^2 / (n_{\text{obs}} - n_{\text{param}})]^{1/2}$.

Table 2. Selected bond lengths (Å) and angles (deg) for complexes **1–3**.

Complex 1			
Cd1–N3	2.292(8)	Cd1–N3	2.258(8)
Cd1–I1	2.6958(12)	Cd1–I2	2.7229(12)
N4–Cd1–N3	106.0(3)	N4–Cd1–I1	108.5(2)
N3–Cd1–I1	100.7(2)	N4–Cd1–I2	105.0(2)
N3–Cd1–I2	108.0(2)	I1–Cd1–I2	127.08(4)
Complex 2			
Cd1–Br1	2.5398(10)	Cd1–Br2	2.5158(9)
Cd1–N3	2.240(4)	Cd1–N1	2.232(4)
Br1–Cd1–Br2	124.76(4)	N3–Cd1–N1	101.19(16)
N3–Cd1–Br1	116.18(13)	N1–Cd1–Br1	100.80(13)
N3–Cd1–Br2	101.51(13)	N1–Cd1–Br2	110.14(12)
Complex 3			
Cd1–N3	2.244(3)	Cd1–N1	2.261(3)
Cd1–Cl1	2.4283(11)	Cd1–Cl2	2.4193(11)
N3–Cd1–N1	103.70(11)	N3–Cd1–Cl2	115.11(9)
N1–Cd1–Cl2	100.92(9)	N3–Cd1–Cl1	108.06(9)
N1–Cd1–Cl1	107.00(9)	Cl1–Cd1–Cl2	120.16(4)

Z = 4. As shown in Fig. 1a, the asymmetric unit of **1** contains one Cd(II) atom, two iodine atoms and one ligand L¹. The Cd(II) center exhibits a distorted tetrahedral geometry and is four-fold coordinated by two nitrogen atoms (N3 and N4) from two L¹ ligands (Cd–N 2.258(8)–2.292(8) Å) and two iodine atoms (I1 and I2) (Cd–I 2.6958(12) and 2.7229(12) Å). The angles around the Cd(II) ion range from 100.7(2) to

Table 1. Crystal data and parameters pertinent to data collection and structure refinement for **1–3**.

127.08(4)°, all in the normal range for analogous complexes [8].

In **1**, the L¹ ligand acts as a bridging bis(monodentate) ligand, in a *cis-trans* conformation and connects CdI₂ units forming a helical chain, in which the dihedral angle between the mean-planes of the two benzimidazole rings in the same L¹ is 63.073°, as shown in Fig. 1b. The distance between two adjacent Cd atoms is 10.7709(4) Å. Two neighboring chains are further connected into a 2D supramolecular network through strong π – π stacking interactions between benzene and imidazole rings from different L¹ ligands with a centroid-to-centroid distance of 3.640(6) Å, as shown in Fig. 1c.

Crystal structure of [CdBr₂(L²)]_n (**2**)

Complex **2** crystallizes in the monoclinic space group *P*2₁/*c* with *Z* = 4. The independent unit consists of one Cd(II) atom, two bromine atoms and one ligand L². The coordination environment of the Cd(II) atom is shown in Fig. 2a. Each Cd(II) atom is four-fold coordinated by two bromine atoms (Br1 and Br2) and two nitrogen atoms (N1 and N3) from two ligands L², with the distances Cd–Br = 2.5158(9) and 2.5398(10) Å and Cd–N = 2.232(4) and 2.240(4) Å. The *cis-*

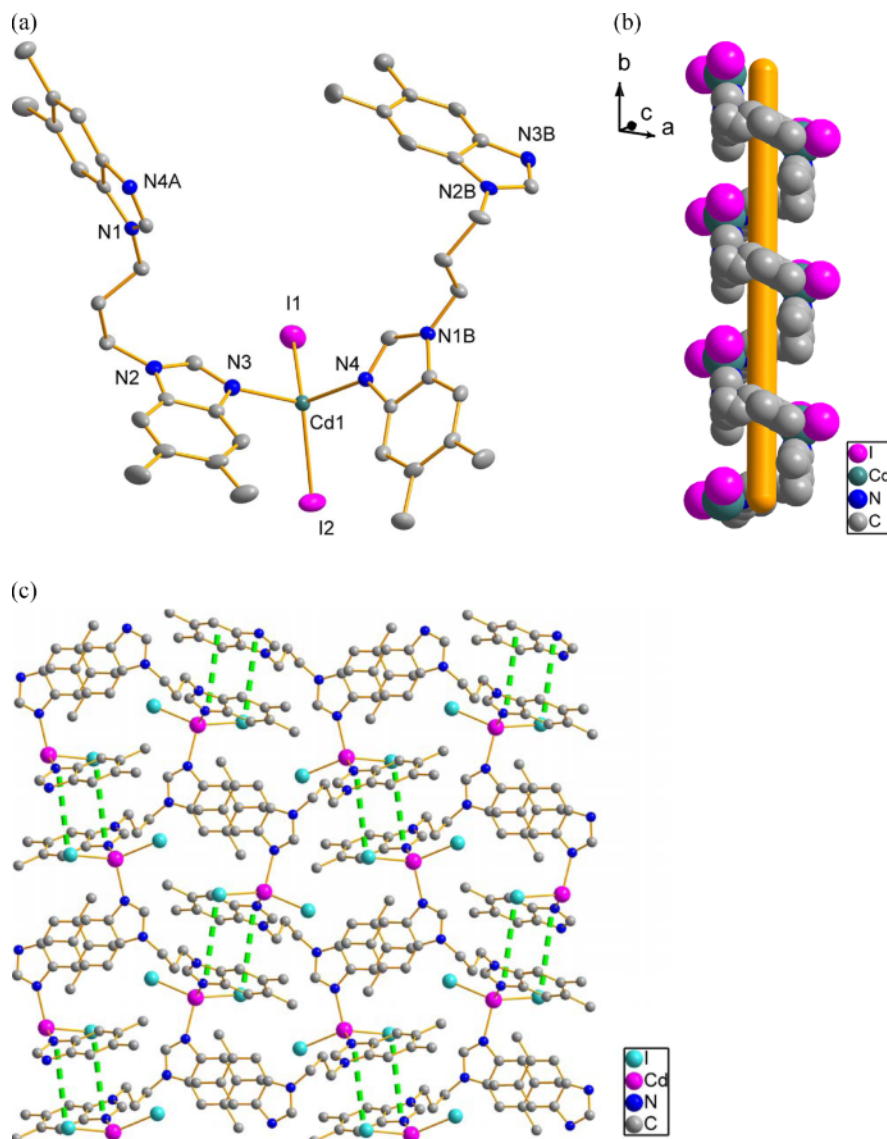


Fig. 1 (color online). (a) Coordination environment around the Cd(II) center in **1**; symmetry transformations used to generate equivalent atoms: A = $-x + 1, y - 0.5, -z + 0.5$; B = $-x + 1, y + 0.5, -z + 0.5$. (b) Helical chain in **1**. (c) 2D supramolecular network connected by π - π stacking interactions in **1**.

coordination bond angles range from $100.80(13)$ to $124.76(4)^\circ$, showing distortion of the tetrahedral geometry in **2**, all in the normal range for related complexes [8].

In **2**, the ligand L^2 is bridging in a bis-monodentate fashion, adopting a *cis-trans* conformation. Different from **1**, the dihedral angle between the mean-planes of the two benzimidazole rings of L^2 is 86.03° . Each

ligand L^2 connects neighboring CdBr_2 units to form a helical chain as shown in Fig. 2b. The distance between two adjacent Cd atoms is $11.3482(6) \text{ \AA}$. These chains are further extended into a 3D supramolecular framework through two kinds of π - π stacking interactions, in which the centroid-to-centroid distances are $3.696(3) \text{ \AA}$ (benzene-imidazole), and $3.472(3) \text{ \AA}$ (imidazole-imidazole), as shown in Fig. 2c.

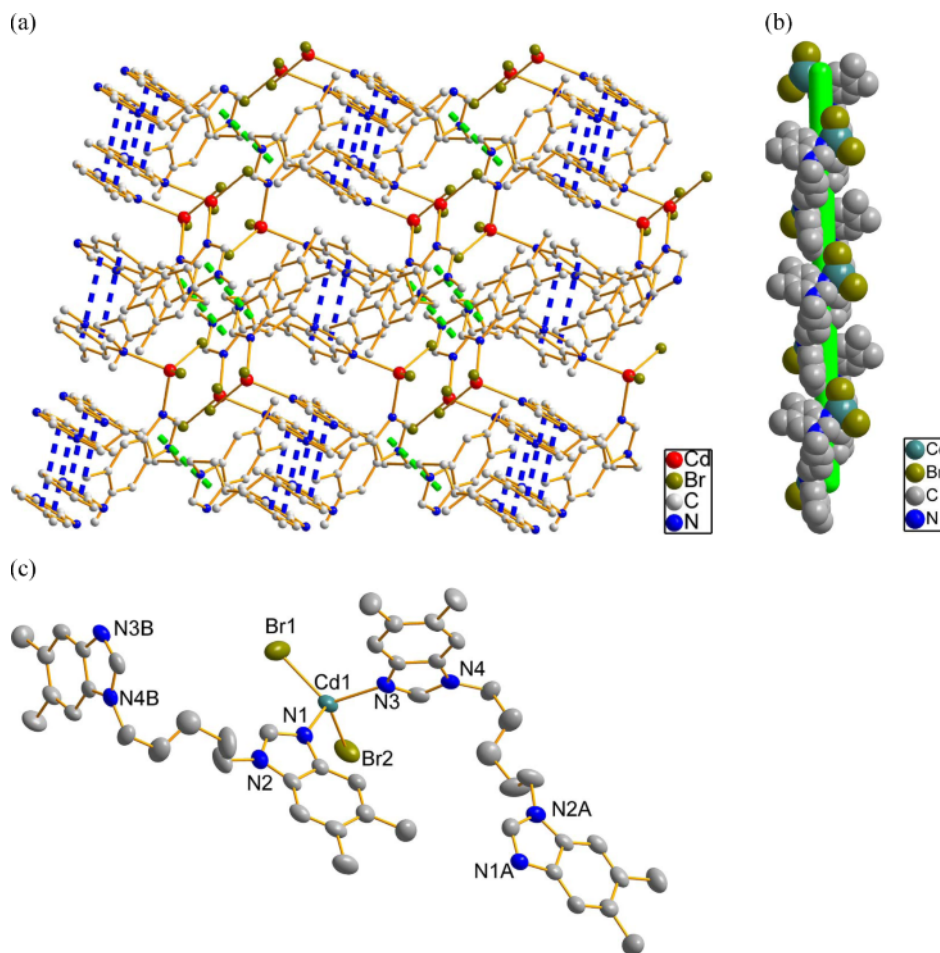


Fig. 2 (color online). (a) Coordination environment around the Cd(II) center in **2**; symmetry transformations used to generate equivalent atoms: A = $-x, y - 0.5, -z + 0.5$; B = $-x, y + 0.5, -z + 0.5$. (b) Helical chain in **2**. (c) 3D supramolecular network connected by π - π stacking interactions in **2**.

Crystal structure of $\text{Cd}_2\text{Cl}_4(\text{L}^3)_2$ (**3**)

Complex **3** exhibits a dinuclear structure. The asymmetric unit of **3** contains one Cd(II) atom, two chlorine atoms and one ligand L^3 . As shown in Fig. 3, the dinuclear complex forms a 26-membered metallomacrocyclic with crystallographically imposed centrosymmetry (monoclinic space group $P2_1/n$ with $Z = 2$). The Cd(II) atoms are four-fold coordinated by two chlorine atoms (Cl1 and Cl2) and two nitrogen atoms (N1 and N3) from two distinct ligands L^3 , showing a distorted tetrahedral geometry. The Cd–N and Cd–Cl bond lengths are 2.244(3), 2.261(3), 2.4193(11), and 2.4283(11) Å, respectively. The corresponding bond angles are be-

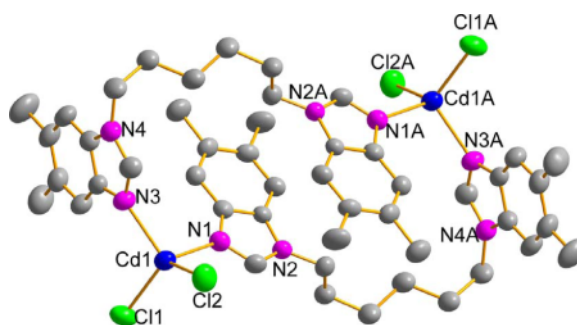


Fig. 3 (color online). Coordination environment around the Cd(II) center in **3**; symmetry transformation used to generate equivalent atoms: A = $-x + 1, -y + 1, -z$.

tween 100.92(9) and 120.16(4)°, all in the normal range for related complexes [8]. In **3**, the ligand L^3 is bridging in a bis-monodentate fashion, and the dihedral angle between the mean-planes of two benzimidazole rings is 79.55°. It adopts a *trans* conformation and connects two neighboring $CdCl_2$ units to form the 26-membered metallomacrocycle with a distance of 10.5045(5) Å between the two Cd(II) atoms.

Structural comparison of **1–4**

Three Cd(II) complexes have been obtained using three structurally related ligands with different spacer lengths $[-(CH_2)_n]$, $n = 3, 5, 6$. Another similar complex $[CdCl_2(L^1)]_n$ (**4**; see Scheme 1) has been previously reported by our group [26]. In **1–4**, the X ($X = Cl, Br, I$) atoms are terminal ligands, and the flexible bis(5,6-dimethylbenzimidazolyl) ligands adopt a bis-monodentate coordination mode but with different conformations (Scheme 1). Different dihedral angles between two benzimidazole rings in the same flexible ligand and long Cd···Cd distances were observed in these complexes. With increasing length of the ligand spacer, the flexibility of L^3 is growing significantly, and its shape becomes curved. The Cd···Cd distance in **3** is 10.5045(5) Å, which is even shorter than that in **1** and **4** bridged by the shortest spacer L^1 (10.7709(4) Å for **1**, 10.7673(6) Å for **4**). Thus the flexible ligands are capable to adjust their configurations to meet the requirements for coordination. Finally the complexes show different architectures: **3** displays a dinuclear metallomacrocylic structure, while **1**, **2** and **4** show chain structures connected by the bis(5,6-dimethylbenzimidazole) ligands. Due to the existence

of strong π – π stacking interactions, **1** and **2** are further extended to 2D and 3D supramolecular structures, respectively. These π – π stacking interactions help to stabilize the crystal structure [27]. Accordingly, the spacer length of flexible ligands and the supramolecular interactions play an important role in the construction of coordination architectures.

IR spectroscopy

The strong bands at 1510 cm^{-1} in **1**, **2** and **3** can be assigned to the $\nu(C=N)$ absorption in the imidazole ring. The presence of bands at 3080 and 2930 cm^{-1} for **1**, 3100 and 2940 cm^{-1} for **2**, and 3100 and 2930 cm^{-1} for **3**, can be considered as $\nu(C-H)$ of $-CH_3$ and $-CH_2-$ of bis(5,6-dimethylbenzimidazole) ligands.

Thermal properties

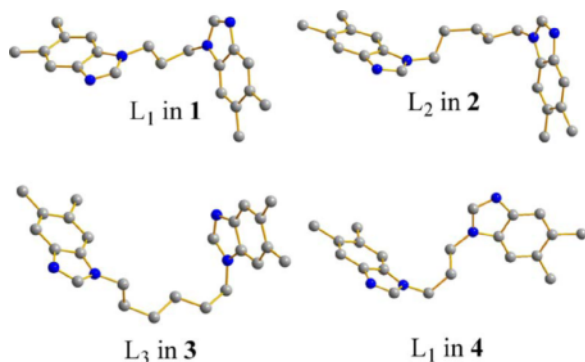
Thermogravimetric analyses were performed to assess the thermal stabilities of **1–3**. The TG curves indicate that the three complexes have excellent thermal stability: **1** and **3** were stable up to 365 °C, and **2** did not collapse up to 405 °C.

Fluorescence properties

The fluorescence properties of **1–3** and their free ligands L^1 – L^3 were studied in the solid state at room temperature (Fig. 4a–c). The ligands all show intense emissions at 370 ± 5 nm upon excitation at 320 nm. Complex **1** shows an emission band at 312 nm upon excitation at 280 nm compared to 372 nm for **2** and 355 nm for **3** upon excitation at 320 nm. Compared with their corresponding free ligands, the emission peaks are blue-shifted 56 nm for **1**, and 11 nm for **3**, which may be due to the ligand-to-metal charge transfer (LMCT) [23, 28–30]. Such an emission of **2** can be tentatively assigned to the intraligand transition of the ligand L^2 [372 nm ($\lambda_{ex} = 320$ nm)] since a similar emission was observed for the free ligand [31].

Conclusion

Three Cd(II) complexes based on flexible α, ω -bis(benzimidazolyl)alkanes have been synthesized hydrothermally. Structure analysis has indicated that the spacer length of flexible ligands and the supramolecular interactions play an important role in the formation



Scheme 1 (color online). Conformations of ligands in the cadmium complexes **1–4**.

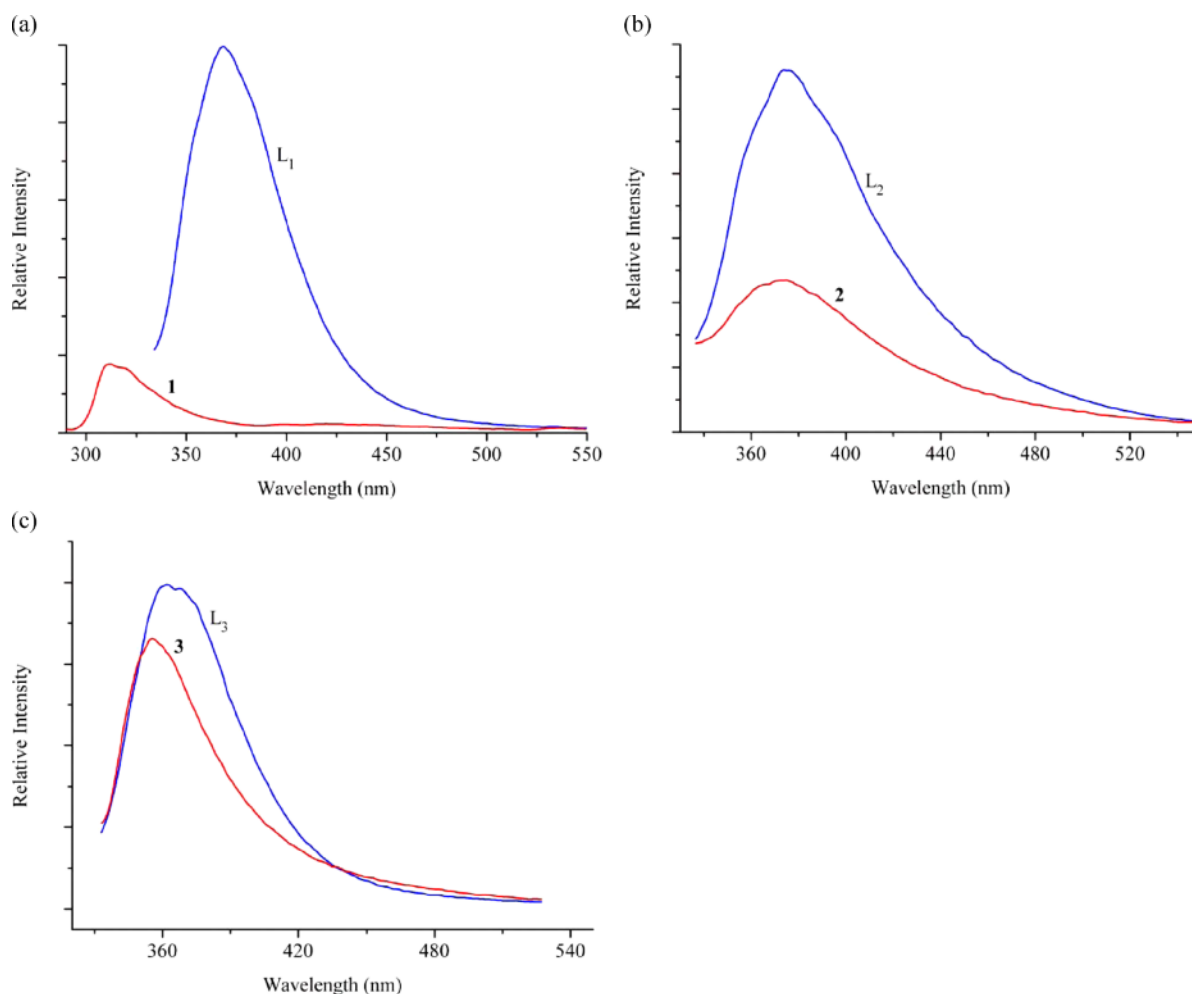


Fig. 4 (color online). (a) Fluorescence emission spectra of the ligand L^1 and complex **1**. (b) Fluorescence emission spectra of the ligand L^2 and complex **2**. (c) Fluorescence emission spectra of the ligand L^3 and complex **3**.

of the different architectures. The TG study revealed that **1–3** are stable up to nearly 400 °C. In addition, they all are fluorescent in the solid state.

Experimental Section

Materials and general methods

All reagents were from commercial sources and of analytical grade and used without further purification. The ligands L^1 – L^3 were prepared according to literature methods [32]. Elemental analyses were obtained on a Perkin-Elmer automatic analyzer. IR spectra were recorded on a Nicolet FT-IR Avatar 360 spectrophotometer in the 4000–400 cm^{-1} region

using KBr pellets. The TG measurements were carried out on a Netzsch TG 209 thermal analyzer from room temperature to 800 °C under N_2 with a heating rate of 10 °C min^{-1} . The fluorescence spectra were performed with a Hitachi F-7000 fluorescence spectrophotometer at room temperature.

Synthesis of $[\text{CdI}_2(L^1)]_n$ (**1**)

A mixture of $\text{Cd}(\text{NO}_3)_2 \cdot 4\text{H}_2\text{O}$ (15.5 mg, 0.05 mmol), KI (16.6 mg, 0.1 mmol), L^1 (16.6 mg, 0.05 mmol), MeOH (3 mL), and H_2O (3 mL) was placed in a Teflon-lined stainless-steel vessel and heated to 140 °C for 72 h under autogeneous pressure, and then cooled to room temperature at a rate of 5 °C h^{-1} . Colorless crystals of **1** were obtained in 78 % yield based on $\text{Cd}(\text{NO}_3)_2 \cdot 4\text{H}_2\text{O}$. – Analysis

for $\text{C}_{21}\text{H}_{24}\text{I}_2\text{CdN}_4$ (698.64): calcd. C 36.10, H 3.46, N 8.02; found C 36.21, H 3.34, N 8.13 %. – FTIR (KBr pellet, cm^{-1}): $\nu = 3080$ (m), 2930 (m), 1630 (w), 1510 (vs), 1450 (m), 1380 (m), 1270 (w), 1210 (m), 1020 (w), 843 (m).

Synthesis of $[\text{CdBr}_2(\text{L}^2)]_n$ (**2**)

The reaction was carried out with a method similar to that for **1**, using KBr (11.9 mg, 0.1 mmol) and L^2 (18.0 mg, 0.05 mmol) instead of KI and L^1 , respectively. Colorless crystals of **2** were obtained in 72 % yield based on $\text{Cd}(\text{NO}_3)_2 \cdot 4\text{H}_2\text{O}$. – Analysis for $\text{C}_{23}\text{H}_{28}\text{Br}_2\text{CdN}_4$ (632.71): calcd. C 43.66, H 4.46, N 8.85; found C 43.61, H 4.38, N 8.73 %. – FTIR (KBr pellet, cm^{-1}): $\nu = 3100$ (w), 2940 (m), 1630 (w), 1510 (vs), 1470 (m), 1380 (m), 1280 (w), 1210 (m), 1060 (w), 856 (m).

Synthesis of $\text{Cd}_2\text{Cl}_4(\text{L}^3)_2$ (**3**)

The reaction was carried out with a method similar to that for **1** using a mixture of $\text{CdCl}_2 \cdot 1.5\text{H}_2\text{O}$ (11.4 mg, 0.05 mmol), L^3 (18.7 mg, 0.05 mmol), MeOH (4 mL), and H_2O (3 mL). Colorless crystals of **3** were obtained in 48 % yield based on $\text{CdCl}_2 \cdot 1.5\text{H}_2\text{O}$. – Analysis for $\text{C}_{48}\text{H}_{60}\text{Cl}_4\text{Cd}_2\text{N}_8$ (1115.66): calcd. C 51.67, H 5.42, N 10.04; found C 51.61, H 5.56, N 9.93 %. – FTIR (KBr pellet, cm^{-1}): $\nu = 3100$ (m), 2930 (m), 1630 (m), 1510 (vs), 1450 (m), 1380 (m), 1270 (w), 1210 (m), 1060 (w), 850 (m).

Crystal structure determinations

Single crystals suitable for the X-ray measurements of complexes **1–3** were mounted on glass fibers with an epoxy cement. The data collections were carried out on a Bruker Smart 1000 CCD diffractometer with graphite-monochromatized $\text{MoK}\alpha$ radiation ($\lambda = 0.71073 \text{ \AA}$) with ω - 2θ scans at 298 K. Absorption corrections were applied using the program SADABS [33]. The structures were solved by Direct Methods and refined by full-matrix least-squares using the Bruker SHELXTL program package [34]. All non-hydrogen atoms were refined with anisotropic displacement parameters. Hydrogen atoms of water were located in difference Fourier maps, while other hydrogen atoms were included in calculated positions and refined with isotropic displacement parameters riding on the corresponding parent atoms. The crystal size of **1** was small, and the crystal was not of good quality which resulted in a large wR_2 parameter. The final difference Fourier maps were essentially flat. A residual electron-density peak is located near the I2 atom in **1**, but this peak could not be modelled as a disordered iodine position. Thus it may be caused by absorption artefacts or series termination errors. Crystallographic data are summarized in Table 1. Selected bond lengths and angles for **1–3** are listed in Table 2.

CCDC 870437–870439 contain the supplementary crystallographic data for this paper. These data can be obtained free of charge from The Cambridge Crystallographic Data Centre via www.ccdc.cam.ac.uk/data_request/cif.

- [1] H. C. Zhou, J. R. Li, *Nat. Chem.* **2010**, 2, 893.
- [2] G. C. Liu, J. X. Zhang, X. L. Wang, H. Y. Lin, A. X. Tian, Y. F. Wang, *Z. Naturforsch.* **2011**, 66b, 125.
- [3] G. H. Cui, C. H. He, C. H. Jiao, J. C. Geng, V. A. Blatov, *CrystEngComm* **2012**, 14, 4210.
- [4] O. Michael, O. M. Yaghi, *Chem. Rev.* **2012**, 112, 675.
- [5] A. Corma, H. García, F. X. Llabrés i Xamena, *Chem. Rev.* **2010**, 110, 4606.
- [6] S. L. Li, Y. Q. Lan, Y. M. Fu, D. Y. Du, H. Y. Zang, K. Z. Shao, Q. F. Z. M. Su, *Cryst. Growth Des.* **2009**, 9, 1353.
- [7] F. A. Almeida Paz, J. Klinowski, S. M. F. Vilela, J. P. C. Tomé, J. A. S. Cavaleiro, J. Rocha, *Chem. Soc. Rev.* **2012**, 41, 1088.
- [8] X. L. Wang, J. X. Zhang, L. L. Hou, G. C. Liu, H. Lin, A. X. Tian, *J. Coord. Chem.* **2011**, 64, 1177.
- [9] S. W. Jin, D. Q. Wang, *J. Coord. Chem.* **2010**, 63, 3042.
- [10] C. H. Jiao, C. H. He, J. C. Geng, G. H. Cui, *Transition Met. Chem.* **2011**, 37, 17.
- [11] J. C. Geng, L. Qin, X. Du, S. L. Xiao, G. H. Cui, *Z. Anorg. Allg. Chem.* **2012**, 638, 1233.
- [12] X. L. Wang, L. L. Hou, J. W. Zhang, J. X. Zhang, G. C. Liu, S. Yang, *CrystEngComm* **2012**, 14, 3936.
- [13] J. Wang, Z. G. Ren, M. Dai, Y. Chen, J. P. Lang, *CrystEngComm* **2011**, 13, 5111.
- [14] Q. Chang, X. R. Meng, Y. L. Song, H. W. Hou, *Inorg. Chim. Acta* **2005**, 358, 2117.
- [15] X. L. Wang, J. X. Zhang, G. C. Liu, H. Y. Lin, Y. Q. Chen, Z. H. Kang, *Inorg. Chim. Acta* **2011**, 368, 207.
- [16] B. Xiao, H. W. Hou, Y. T. Fan, M. S. Tang, *Inorg. Chim. Acta* **2007**, 360, 3019.
- [17] X. R. Meng, B. Xiao, Y. T. Fan, H. W. Hou, G. Li, *Inorg. Chim. Acta* **2004**, 357, 1471.
- [18] Z. X. Li, X. Chu, G. H. Cui, Y. Liu, L. Li, G. L. Xue, *CrystEngComm* **2011**, 13, 1984.
- [19] X. L. Tang, W. Dou, J. A. Zhou, G. L. Zhang, W. S. Liu, L. Z. Yang, Y. L. Shao, *CrystEngComm* **2011**, 13, 2890.

- [20] S. S. Marwaha, R. P. Sethi, J. F. Kennedy, *Enzyme Microb. Technol.* **1983**, 5, 361.
- [21] S. Y. Zhang, Z. J. Zhang, W. Shi, B. Zhao, P. Cheng, *Inorg. Chim. Acta* **2010**, 363, 3784.
- [22] X. L. Wang, S. Yang, G. C. Liu, L. L. Hou, H. Y. Lin, A. X. Tian, *Transition Met. Chem.* **2011**, 36, 891.
- [23] X. L. Wang, J. X. Zhang, L. L. Hou, J. W. Zhang, G. C. Liu, H. Y. Lin, *J. Chem. Crystallogr.* **2011**, 41, 1579.
- [24] C. H. He, C. H. Jiao, J. C. Geng, G. H. Cui, *J. Coord. Chem.* **2012**, 65, 2294.
- [25] J. C. Geng, L. Qin, C. H. He, G. H. Cui, *Transition Met. Chem.* **2012**, 37, doi:10.1007/s11243-012-9624-1.
- [26] C. H. Jiao, J. C. Geng, C. H. He, G. H. Cui, *J. Mol. Struct.* **2012**, 1020, 134.
- [27] C. Janiak, *J. Chem. Soc., Dalton Trans.* **2000**, 3885.
- [28] X. L. Wang, S. Yang, G. C. Liu, J. X. Zhang, H. Y. Lin, A. X. Tian, *Inorg. Chim. Acta* **2011**, 375, 70.
- [29] M. A. Braverman, R. M. Supkowski, R. L. LaDuca, *J. Solid State Chem.* **2007**, 180, 1852.
- [30] X. L. Wang, Y. F. Bi, H. Y. Lin, G. C. Liu, B. K. Chen, *J. Organomet. Chem.* **2007**, 692, 4353.
- [31] Y. J. Lee, E. Y. Kim, S. H. Kim, S. P. Jang, T. G. Lee, C. Kim, S. J. Kim, Y. Kim, *New J. Chem.* **2011**, 35, 833.
- [32] G. H. Cui, J. R. Li, J. L. Tian, X. H. Bu, S. R. Batten, *Cryst. Growth Des.* **2005**, 5, 1775.
- [33] G. M. Sheldrick, SADABS (version 2.03), Program for Empirical Absorption Correction of Area Detector Data, University of Göttingen, Göttingen (Germany) **1996**.
- [34] G. M. Sheldrick, SHELXTL (version 6.10), Bruker Analytical X-ray Instruments Inc., Madison, Wisconsin (USA) **2001**. See also: G. M. Sheldrick, *Acta Crystallogr.* **2008**, A64, 112.